A New Longitudinal Emittance Monitor for Proton Beams Using Elastic Scattering by a Gold Target

AUTHOR(S):

Dewa, Hideki; Kando, Masaki; Ikegami, Masanori; Shirai, Toshiyuki; Okamoto, Hiromi; Iwashita, Yoshihisa; Fujita, Hirokazu; Kakigi, Shigeru; Noda, Akira; Inoue, Makoto

Bull. Inst. Chem. Res., Kyoto Univ., Vol. 73, No. 1, 1995

A New Longitudinal Emittance Monitor for Proton Beams Using Elastic Scattering by a Gold Target

Hideki DEWA*, Masaki KANDO*, Masanori IKEGAMI*, Toshiyuki SHIRAI*, Hiromi OKAMOTO*, Yoshihisa IWASHITA*, Hirokazu FUJITA*, Shigeru KAKIGI*, Akira NODA* and Makoto INOUE*

Received February 9, 1995

A new method for monitoring the longitudinal phase-space of proton beams is proposed. The protons scattered by a narrow and thin gold target on a beam line are deflected by RF electric field with proper phases. Then the deflected protons are detected by a position sensitive detector. The original longitudinal phase-space distribution can be deduced from the energies and positions measured by the detector. The measurable range of the longitudinal phase spread is less than $\pm 60^\circ$ around synchronous phase. The resolutions of the energy and phase are 40 keV and 3.8° respectively. We plan to fabricate this new monitor for the investigation of longitudinal dynamics of the ICR linac.

KEY WORDS: Bunch monitor/ Longitudinal emittance/ Phase distribution/ Energy distribution/ RF deflector

1. INTRODUCTION

For better understandings of the dynamical properties of the beam in an accelerator, it is important to know the phase-space distribution of the output beams. An ordinary emittance monitor can provide the transverse information. The phase and energy spread of the beam should be measured simultaneously for the longitudinal phase-space information. In the measurement of longitudinal emittance of the beams accelerated in a high frequency linac, very high time resolution is required.

For H^- ion beams, the laser-induced neutralization method has been studied in Los Alamos National Laboratory[1,2]. A portion of H^- beams can be selectively neutralized by a short pulsed laser and the neutralized part is separated from the other part by a dipole magnet. The energy of the neutralized beams is measured either by the time-of-flight or by a spectrometer, while the phase is evaluated by changing the phase of the laser pulse relative to the RF phase of the accelerator.

Another method for the longitudinal emittance measurement for H^- beams was recently proposed[3]. In this method, an electron photo-detached from an H^- ion by a short pulsed laser is employed, as well as the previous method, to determine the ion energy under the assumption that the velocity of the electron is approximately equal to that of the ion. Since the electron mass is much smaller than the ion mass, one can measure the electron velocity with small spectrometer compared with that for the previous method.

* 出羽秀紀, 神門正城, 池上雅紀, 白井敏之, 岡本宏巳, 岩下芳久, 冨士田浩一, 柿木 茂, 野田 章, 井上 信 : Nuclear Science Research Facility, Institute for Chemical Research, Kyoto University.

A bunch shape monitor using the secondary electrons emitted through collisions of the ion beams and a thin wire is also reported[4,5]. The emitted electrons are accelerated by high DC voltage and then deflected by the RF electric field synchronous to the RF of linac. Electrons within a narrow phase range are detected after passing through a slit. The phase distribution can thus be obtained by shifting the phase of the deflection RF. Although this method has a good resolution, the energy distribution cannot be measured.

For a systematic study of longitudinal dynamics, we plan to measure the longitudinal emittance of the 7 MeV Alvarez linac at ICR operating at 433 MHz. The pulsed laser methods can, however, be applied only to negative ions while the ICR linac accelerates protons. We here describe a possible new method for measuring the longitudinal phase-space of proton beams. The accuracy of the measurement based on the present method is also estimated in this paper.

2. MEASUREMENT SYSTEM

The system considered here consists of a narrow gold target, a slit, an RF cavity for deflecting the protons scattered by the target, and a position sensitive detector (PSD). The schematic view is shown in Fig. 1. The narrow and thin gold target is located on the beam line. The proton elastically scattered by the target at the angle of 90° goes through the slit. Taking into account the scattering cross section and the slit width, it is anticipated that the burst counting rate is about one thousand counts per second. This counting rate is low enough to reduce the pile-up effect and the dead time of A/D converter. The proton is then deflected in the RF cavity. The deflection angle depends on the kinetic energy and the timing when it traverses

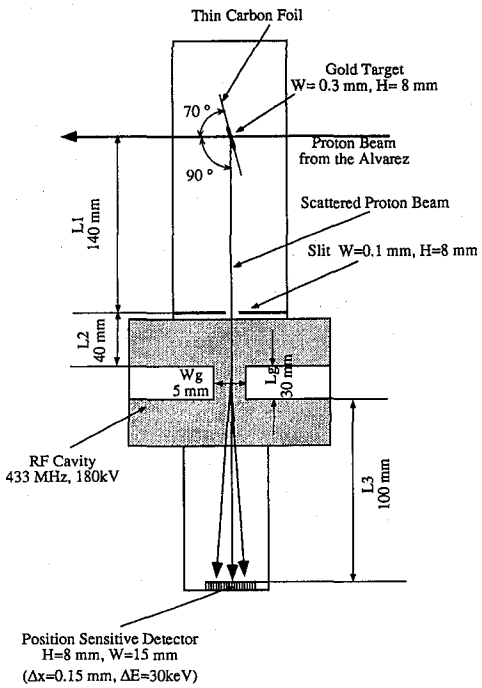

Fig. 1. Schematic view of the longitudinal emittance monitor.

the cavity. The energy and position of the deflected proton are measured with the PSD, in order to derive its energy and relative phase before the scattering. Thus the accumulated information for enough time, typically 250 seconds, enables us to reconstruct the original phase-space distribution of the proton beams.

Let us now take a look at the motion of a scattered proton having the relative phase $\Delta\phi$ and the velocity βc. We here assume that the synchronous particle with the velocity $\beta_0 c$ is scattered at $t=0$. The phase of the deflection RF is adjusted such that the synchronous proton scattered exactly by 90° traverses the central point of the electrodes at the zero phase. Then, for a non-synchronous particle passing by the electrodes at t_1, the transverse velocity $v(t_1)$ and the position $x(t_1)$ are evaluated as

$$\begin{aligned} v(t_1)&=\frac{2qV}{mW_g\omega}\sin\left\{\Delta\phi+\frac{\omega(L_1+L_2+L_g/2)}{c}\left(\frac{1}{\beta}-\frac{1}{\beta_0}\right)\right\}\sin\left(\frac{\omega L_g}{2\beta c}\right),\\ x(t_1)&=-\frac{qV}{mW_g\omega^2}\cos\left\{\Delta\phi+\frac{\omega}{c}(L_1+L_2+L_g/2)\left(\frac{1}{\beta}-\frac{1}{\beta_0}\right)\right\}\sin\left(\frac{\omega L_g}{2\beta c}\right)\\ &\quad+\frac{qV}{mW_g\omega}\cos\left\{\Delta\phi+\frac{\omega(L_1+L_2)}{\beta c}-\frac{\omega(L_1+L_2+L_g/2)}{\beta_0 c}\right\}\frac{L_g}{\beta c}, \end{aligned} \tag{1}$$

where q is the elementary electric charge, V is electrode gap voltage, m is the mass of proton, W_g is gap width of the electrodes, and ω is RF angular frequency. In this calculation, the RF field distribution between the electrodes is assumed to be uniform. The transverse velocity and position on the PSD are given by

$$\begin{aligned} v(t_2)&=v(t_1),\\ x(t_2)&=x(t_1)+v(t_1)\frac{L_3}{\beta c}, \end{aligned} \tag{2}$$

where t_2 is the time when the proton considered arrives at the PSD.

It is clear that the phase dependence of the detected position is not linear, and further more is a function of the proton energy. To obtain the original phase and energy, Eq. (2) together with Eq. (1) must be solved based on the measurement results for the $v(t_2)$ and $x(t_2)$. Note that, if the distance between the target and electrodes is too long, the phase error caused by the finite energy spread of scattered beam affects the measurement accuracy considerably. For example, in order to have the error less than 10° with the energy spread of 200 keV, $L_1+L_2+L_g/2$ must be shorter than 16 cm.

2.1 *Gold target*

The target is deposited on a thin carbon foil by means of vacuum evaporation. Gold is appropriate for the target material because of its large scattering cross section. Although most of the beam transit only the carbon foil, some are scattered at the narrow gold target after the carbon foil. Because the proton transfers energy to the gold nucleus in the elastic scattering process, the kinetic energy of 7.00 MeV proton scattered by 90° decreases to 6.93 MeV.

The phase resolution depends on the size of the deposited gold strip, which is 0.3 mm wide and 8 mm high in our case. The height is taken to be the same as that of the PSD. A larger tilting angle of the target is preferable for making the target projection size viewed from the electrode region as small as possible. In our case, the target is set on the beam line with the 70°

tilting angle, corresponding the projection size of 0.1 mm×8 mm.

The thicknesses of the gold and carbon should be determined in consideration of the ionization loss. Because the ionization loss during the scattering process depends on the path length in the target and thus causes an error in energy measurement, the gold deposition should be as thin as possible. We require the thickness of gold to be 0.1 μm corresponding to the mean ionization of 4.9 keV evaluated from the Bethe-Bloch formula. The mean ionization loss for the longest path in the gold is 14.4 keV, and that for the shortest path is 5.2 keV. Therefore the energy measurement spread by the different path in the gold target is 9.2 keV.

The ionization loss in the carbon foil is about 0.6 keV, much smaller than that in the gold target, when the thickness of the carbon foil is 10 μg/cm^2. The scattering probability in the carbon foil is only 0.46% of that for the gold target. However, assuming a round beam with 10 mm in diameter, the number of the protons scattered by the carbon is expected, in our case, to be about 15% of those coming from the gold target because of the target size smaller than the beam size. But the kinetic energy of a 7 MeV proton scattered by the gold target is about 6.93 MeV, while that by the carbon foil is about 5.91 MeV. Therefore it is easy to separate the background signals originating from the carbon scattered protons.

2.2 *Slit*

The solid angle of the slit affects the counting rate and the resolution of position measurement. High counting rate and high resolution are not compatible. In addition, the finite distance between the target and the slit results in an undesirable shift of the deflector phase as mentioned before. In our case, the slit width and the distance between the target and the slit are 0.1 mm and 140 mm respectively. The detailed estimations of the resolution are described in Section 2.6. The slit height is 8 mm, the same as that of PSD.

In order to suppress the scattering at slit edge, a thin slit made of short range material is preferable. Because the slit is made of tantalum whose range is about 0.115 mm for 7 MeV proton, the thickness of 0.2 mm should be enough to stop the scattered protons. The probability of scattering at the slit edge is less than 0.2% of all transitions through the slit, when the distance from the target is 140 mm.

2.3 *RF deflector*

The scattered protons are deflected by strong electric field produced in an RF cavity, synchronized with the linac RF. As mentioned, the deflector phase is adjusted such that the synchronous particle is not deflected. Since the electrodes effective length must be shorter than $\beta\lambda/2 \approx 41.8$ mm for a 6.93 MeV proton, about 30 mm of effective length may be appropriate. Because of the sinusoidal change of the deflection voltage, the usable range of the RF phase is less than $\pm 90^\circ$ around the zero phase where we have a monotonic increase (or decrease) of the voltage. Although a sawtooth wave is preferable to the sinusoidal wave due to its linearity, high-frequency sawtooth RF with a high voltage is difficult to generate. The nonlinearity of the sinusoidal wave may limit the reliable measurement region less than $\pm 60^\circ$. The maximum deflection angle is $\pm 3.6^\circ$ assuming the gap voltage of 180 kV and the electrode distance of 5 mm.

2.4 *Position sensitive detector (PSD)*

We can measure the position and energy of a charged particle by a PSD (IPP 1508, Oxford Instruments Inc.) simultaneously. The detection area is 15×8 mm^2, and the position can be

measured along one dimension of 15 mm width. The position resolution is 0.15 mm, and the energy resolution is 30 keV. Therefore total energy error including the effect of ionization loss in the gold target is less than 40 keV. The distance from the RF electrodes determines the phase resolutions. The distance of 100 mm is enough for good phase resolution. Lead shields against X-rays, which come from accelerator tank, are considered to be installed around the detector.

2.5 *Simulation*

As an example, let us consider a bunch having a uniform longitudinal phase-space distribution with a rectangular boundary. The phase spread is $\pm 90°$ around the synchronous value, and the energy spread is ± 0.2 MeV around the central value 7.0 MeV. 209 particles are distributed inside the boundary with the 10° phase step and 20 keV energy step. The corresponding position and energy detected on the PSD for each particle are plotted in Fig. 2.

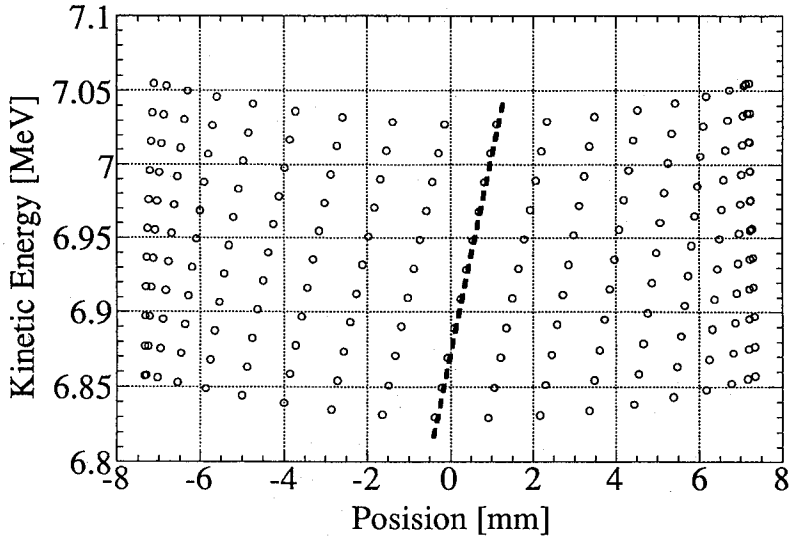

Fig. 2. Calculation of the positions and energies on the PSD for the protons whose energies are from 6.9 MeV to 7.1 MeV and phases are within $\pm 90°$. The circles on dashed line correspond to the particles at the synchronous phase.

The effects originating from three different sources of nonlinearity can be observed in Fig. 2. The first source is concerned with the nonlinearity in the sinusoidal RF wave. It is clear from the figure that the density of the detected particles becomes higher near the left and right edge. This implies that the resolution at the larger deflection angle is lower.

The second source comes from the phase slip of the deflector RF caused by the beam energy spread described before. Two protons which have the same longitudinal displacements but different kinetic energies will get different deflection angles due to this effect. As a result, they will arrive at different positions on the PSD. The circles on the dashed line in Fig. 2 correspond to the particles at the synchronous phase with different energies. The third source is transverse energy gain in the deflector. The slight energy increase in both right and left margins in Fig.2 indicates this effect.

2.6 *Measurement errors*

The accuracy of phase measurement is related to various factors; namely the target width and thickness, the slit width, RF voltage of the deflector, the PSD property, and the geometry of the system. Even protons with the same acceleration phase and energy may reach different points on the PSD, because of the finite beam size and the finite slit width. We evaluated the possible maximum position spread on the PSD for these protons, considering different scattering positions and scattering angles. This calculation includes the effect of phase shifts in the deflector RF caused by the different path lengths. Converting the calculated position spread into error in the acceleration RF phase, we obtain Fig. 3 demonstrating that the error due to a finite beam size is less than 3.0° within the phase of ±50°, but it increases for a larger phase.

Other measurement errors come from the position and energy resolution of the PSD. The phase errors based on these factors are also plotted in Fig. 3. The error due to the position resolution is no more than 2° within the phase of ±50°, while that due to the energy resolution of 40 keV increases monotonically.

The total phase error is estimated by taking the root mean square of the three errors. As seen from Fig. 3, the protons within the phase range of ±60° around the synchronous one can be measured with the phase error less than 6°. Since actual accelerated beam have been well bunched around the synchronous phase, the typical error in phase measurement should be 3.8°.

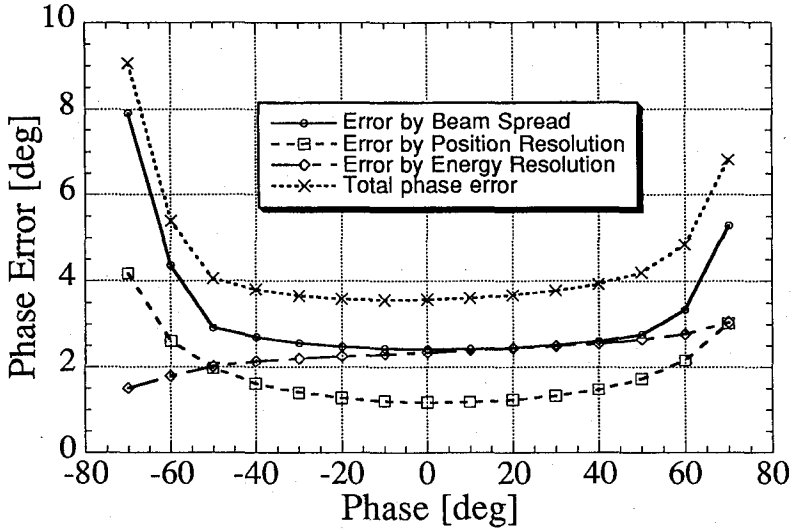

Fig. 3. Phase measurement error caused by three factors; scattering proton beam spread, position resolution of PSD, energy resolution of PSD. Total error is estimated by mean square root of three errors.

3. DATA TAKING SYSTEM

For data taking and data analysis, we consider the following system. We can get, from the PSD, two signals for a single scattered particle; namely, an energy signal and a position signal. These signals have to be amplified by low noise pre-amplifiers and are then transferred to control room. The signals are further amplified and converted to digital signals with 12 bit A/D converters. The digital signals are stored in a computer. The measurement time is estimated

about 250 seconds in order to accumulate 1000 data points, when the average beam current is 4.5 μA.

4. SUMMARY

A new idea for longitudinal emittance measurement is proposed. The longitudinal phase-space of proton beams consisting of 433 MHz micro bunches could be probed with the phase resolution of 3.8° and energy resolution of 40 keV. The resolution depends essentially on the PSD property and the geometry of the monitor system. Further study including a detailed design is going on.

REFERENCES

(1) W.B. Cottingame, G.P. Boicourt, J.H. Cortez, W.W. Higgins, O.R. Sander, and D.P. Sandval, "Noninterceptive Techniques for the Measurement of Longitudinal Parameters for Intense H^- Beams", *IEEE Trans. on Nucl. Sci.*, Vol. **NS-32**, No. 5, 1871–1873, October (1985).

(2) R.C. Connolly and D.P Sandoval, "A Real-Time Longitudinal Phase-Space Measurement Technique for H^- Beams", Proc. 1991 IEEE Particle Accelerator Conference, Vol. **2**, pp. 1237–1239 (1991).

(3) K. Shindo and Y. Mori, "A New Scheme for Measuring the Longitudinal Emittance of Negative Ion Beams", Proceeding of the 19 th Linear Accelerator Meeting in Japan, pp. 111–114 (1994) (in Japanese).

(4) A.V. Feschenko, P.N. Ostroumov, "Bunch Shape Measuring Technique and its Application for an Ion Linac", Proc. 1986 Linac conference, pp. 323–327 (1986).

(5) Elliott S. McCrory and Charles W. Schmidt, "Use of an INR-style Bunch-Length Detector in Fermilab Linac" Proc. 1992 Linear Accelerator Conference, Vol. **2**, pp. 662–664 (1992).